Magnetic fields and the outer rotation curve of M31

B. Ruiz-Granados and J.A. Rubiño-Martín
Instituto de Astrofísica de Canarias (IAC), E-38200, La Laguna, Tenerife (Spain)
and
Departamento de Astrofísica, Universidad de La Laguna, E-38205, La Laguna, Tenerife (Spain)

E. Florido and E. Battaner
Departamento Física Teórica y del Cosmos. Universidad de Granada, Granada(Spain)
and
Instituto de Física Teórica y Computacional Carlos I, Granada(Spain)

ABSTRACT

Recent observations of the rotation curve of M31 show a rise of the outer part that can not be understood in terms of standard dark matter models or perturbations of the galactic disc by M31's satellites. Here, we propose an explanation of this dynamical feature based on the influence of the magnetic field within the thin disc. We have considered standard mass models for the luminous mass distribution, a NFW model to describe the dark halo, and we have added up the contribution to the rotation curve of a magnetic field in the disc, which is described by an axisymmetric pattern. Our conclusion is that a significant improvement of the fit in the outer part is obtained when magnetic effects are considered. The best-fit solution requires an amplitude of ~ 4 μG with a weak radial dependence between 10 and 38 kpc.

Subject headings: galaxies: individual (M31) , galaxies: magnetic fields

1. Introduction

Recent high sensitivity measurements of the rotation curve of M31 (Chemin et al. 2009; Corbelli et al. 2010, hereafter C09 and C10 respectively) suggest that it highly rises at the outermost part of the disc of M31 ($r \gtrsim 25 - 30$ kpc) (see Figure 1). This behaviour cannot be considered an exception. Similar outer rising rotation curves can be found in other galaxies. Noordermeer et al. (2007) stated that "in some cases, such as UGC 2953, UGC 3993 or UGC 11670 there are indications that the rotation curves start to rise again at the outer edges of the HI discs", suggesting follow-up observations of higher sensitivity to investigate this fact in more detail. Other examples could be found in some rotation curves provided by Spano et al. (2008), in particular the curves of UGC 6537 (SAB(r)c), UGC 7699 (SBcd/LSB), UGC 11707 (Sadm/LSB) or UGC 11914 (SA(r)ab) measured by means of Fabry-Perot spectroscopy. Other potential examples could be NGC 1832 and NGC 2841 (Kassin et al. 2006), even with a larger error, and ESO 576-G51 and ESO 583-G7 (Seigar et al. 2005), even if the outer rising is small. Potential nearby candidates could be NGC 3198, DDO 154 or NGC 7331 (de Blok et al. 2008). Therefore, outer rising rotation curves are not uncommon in spirals, being the case of M31 the most representative. This puzzling dynamic feature requires a theoretical explanation. A detailed study by C09 showed that the NFW, Einasto or pseudo-isothermal dark matter halos fail to reproduce the exact shape of the rotation curve of M31 in the outer region and found no differences between the various halo shapes. Moreover, they found new HI structures as an external arm and thin HI spurs in the outskirts of the disc. These spurs have been also observed by Braun et al. (2009). Thus, a primarily explanation of this gas perturbations

could be the interactions with the M31's satellites as NGC 205 (Geehan et al. 2006; Corbelli et al. 2010). The main problem of matching the properties of the giant stellar stream observed in the south of M31 (Ibata et al. 2001) is that the orbital of the companion that produce the stream is not constrained satisfactorily (Fardal et al. 2006) or high velocities for the radial orbits are found (see e.g. Howley et al. 2008). Although the northeastern (NE) and southwestern (SW) parts of M31 show different kinematical properties, both suggest a rise in the outer part of the rotation curve (see Figure 5 and 6 in C09 and C10, respectively).

In this work, we show that magnetic dynamic effects constitute a clear and simple basis to interpret this feature. Some particular models of magnetically driven rotation curves have been presented (Nelson 1988; Battaner et al. 1992; Battaner & Florido 1995, 2000, 2007; Kutschera & Jalocha 2004; Tsiklauri 2008). Although those models were originally developed to explain flat rotation curves without dark matter, our purpose here is more conventional and we will consider the contribution of both a NFW dark matter halo and a magnetic field added to match the velocity in the outermost region.

Magnetic fields are known to slowly decrease with radius (see e.g. Beck et al. 1996; Han et al. 1998; Beck 2001, 2004, 2005), and therefore they become increasingly important at the rim. For large radii, an asymptotic $1/r$-profile for the field strength provides an asymptotic vanishing magnetic force. This $1/r$-profile has been found to match the polarized synchrotron emission of the Milky Way (Ruiz-Granados et al. 2010) and NGC 6946 (Beck 2007), and will be considered in this work.

2. Mass models and the magnetic field of M31

In this section, we briefly present the luminous and dark mass models used to describe the observational rotation curve of M31. As we are interested in the outer region (i.e. distances higher than 10 kpc), we follow C10 and we neglect the bulge contribution. We will also adopt from C09 and C10 the parameters describing stellar disc and gaseous distribution, respectively. Therefore, we will only leave as free parameters those describing two physical components: the dark matter halo and the magnetic field.

2.1. Disc model

The stellar disc is assumed to be exponential (Freeman 1970), being the surface mass density

$$\Sigma = \Sigma_0 \exp\left(\frac{-r}{R_d}\right), \tag{1}$$

where Σ_0 is the central density of stars and R_d, the radial scale factor.

The contribution to the circular velocity of the stellar disc is (see Binney & Tremaine 1987)

$$v_d(r) = 4\pi G\Sigma_0 R_d y^2[I_0(y)K_0(y) - I_1(y)K_1(y)], \tag{2}$$

where $y = r/2R_d$ and I_0, K_0, I_1, K_1 are the modified Bessel's functions for first and second order.

The gaseous disc mainly contains HI, molecular gas and helium. The estimated gaseous distribution of M31 represents approximately a 9% (for C09) and 10% (for C10) of the total mass of the stellar disc (see Table 1).

For the spatial distribution of the gas, we again assume the same exponential law given by Equation (1).

2.2. Halo model

The dark matter halo is described here by a NFW profile (Navarro et al. 1996)

$$\rho_h(r) = \frac{\delta_c \rho_c}{\frac{r}{R_h}\left[1 + \left(\frac{r}{R_h}\right)\right]^2}, \tag{3}$$

where δ_c is a characteristic density contrast, $\rho_c = 3H_0^2/8\pi G$ is the critical density and R_h is the radial scale factor. The contribution to the circular velocity due to this profile is given by (Navarro et al. 1997)

$$v_h(x) = V_{200}\sqrt{\frac{1}{x}\frac{\ln(1+cx) - \frac{cx}{1+cx}}{\ln(1+c) - \frac{c}{1+c}}}, \tag{4}$$

where V_{200} is the velocity at the virial radius R_{200} which is assumed ~ 160 kpc for C09 and $R_{200} \sim 200$ kpc for C10, c is the concentration parameter of the halo which is defined as $c = R_{200}/R_h$ and x is r/R_{200}. According to C09 and C10, the total dark halo mass at the respective virial radius is

$M_{200} \sim 10^{12}\ M_{\odot}$. Our free parameters are V_{200} and c. Values from C09 are $c = 20.1 \pm 2.0$ and $V_{200} = 146.2 \pm 3.9\ km/s$. Values from C10 are $c = 12$ and $V_{200} \sim 140\ km/s$.

2.3. The regular magnetic field of M31

The first measurements of the magnetic field of M31 were obtained by Beck (1982) using the polarized synchrotron emission at 2700 MHz, showing that a magnetic pattern was aligned with HI structures and formed a ring at $r \approx 10$ kpc. They obtained a strength of $B_{reg} = 4.5 \pm 1.2\ \mu$G. Berkhuijsen et al. (2003) used observations of polarized emission to show that M31 hosts an axisymmetric field. Han et al. (1998) used Faraday rotation measurements to show that the regular field could extend at least up to galactocentric distances of $r \sim 25$ kpc without significant decrease of the strength and at least with a $z \sim 1$ kpc of height above the galactic plane. However, recently, Stepanov et al. (2008) have shown that these results contained a significant contribution of Galactic foregrounds and so, it is difficult to infer the model from these measurements. In any case, as we show below, the detailed structure of the field is not relevant for the rotation curve.

Fletcher et al. (2004) presented a detailed study of the regular field of M31 based on multi-wavelength polarized radio observations in the region between 6 and 14 kpc. By fitting the observed azimuthal distribution of polarization angles, they found that the regular magnetic field follows an axisymmetric pattern in the radial range from 8 to 14 kpc. The pitch angle decreases with the radial distance, being $p \sim -16^{\circ}$ for distances $r < 8$ kpc, and $p \sim -7^{\circ}$ for $r < 14$ kpc. This fact implies that the field becomes more tightly wound with increasing galactocentric distance. They found a total field strength (i.e. regular and turbulent components) of $\approx 5\ \mu$G. For the regular field they found that it became slowly lower, reaching at $r \sim 14$ kpc a strength of $\sim 4.6\ \mu$G.

In this paper, our basic assumption is that the regular magnetic field of M31 is described by an axisymmetric model, that extends up to 38 kpc. For this model, the components in cylindrical coordinates are given by

$$B_r = B_0(r)\sin(p) \quad (5)$$

$$B_\phi = B_0(r)\cos(p), \quad (6)$$

where p is the pitch angle and $B_0(r)$ is the field strength as a function of the radial distance. As shown below, from the point of view of the description of the rotation curve, the relevant component is B_ϕ. Here, we will assume that $p = 0^{\circ}$, as we are mostly interested in the outer region where p is very low. Several previous probes also indicates low values of p. In any case, this is not a strong assumption in the sense that a non-zero p value can be absorbed into the field strength (B_1) as a different amplitude. For the field strength, as a baseline computation, we shall consider a radial dependence of $B_0(r)$ or equivalently B_ϕ given by

$$B_\phi(r) = \frac{B_1}{1 + \frac{r}{r_1}}, \quad (7)$$

where r_1 represents the characteristic scale at which $B_0(r)$ decreases to half its value at the galactic centre and B_1 is an amplitude in which we are absorbing the $\cos(p)$ factor. This expression has an appropriate asymptotic behaviour, in the sense that we obtain a finite value when r is close to the galactic center ($r \to 0$), and asymptotically tends to $\propto 1/r$ when $r \to \infty$, as suggested Battaner & Florido (2007). Observations carried out by Fletcher et al. (2004) established that

$$B_\phi(r = 14kpc) \approx 4.6\mu G. \quad (8)$$

This observational value at this radius was considered as fixed in our baseline computation. By substituting into Equation (7), we can find a relation between B_1 and r_1 that allows us to re-write Equation (7) in terms of a single free-parameter (r_1)

$$B_\phi(r) = \frac{4.6 r_1 + 64.4}{r_1 + r}, \quad (9)$$

where r is given in kpc and $B_\phi(r)$ in μG.

3. Methodology

3.1. Observational rotation curve of M31

We have considered the two datasets from C09 and C10. They consist on a set of 98 and 29 measurements of the circular velocity (and their associated error bars) respectively, which were obtained with the high-resolution observations performed with the Synthesis Telescope and the 26-m antenna at the Dominion Radio Astrophysical Observatory (C09) and with the wide-field

and high-resolution HI mosaic survey done with the help of the Westerbork Synthesis Radiotelescope and the Robert C. Byrd Green Bank Telescope (GBT) (Braun et al. 2009). For our purposes, we consider only distances higher than $r > 10$ kpc to illustrate the effects of the magnetic field. The actual data points on the rotation curve were obtained after fitting a tilted ring model to the data, and assuming a distance to M31 of 785 kpc. C09 derived a value of the inclination angle of $i \sim 74°$, which is lower than that derived from optical surface photometry measurements (Walterbos & Kennicutt 1987) and by C10 ($i \sim 77°$). The data points are plotted in Figure 1, in two separate panels.

3.2. Influence of the magnetic field on the gas distribution

The presence of a regular magnetic field affects the gas distribution (Battaner et al. 1992; Battaner & Florido 1995, 2000). The fluid motion equation can be written as (see e.g. Battaner 1996)

$$\rho\frac{\partial\vec{v}_0}{\partial t}+\rho\vec{v}_0\cdot\vec{\nabla}\vec{v}_0+\vec{\nabla}P = n\vec{F}+\frac{1}{4\pi}\vec{B}\cdot\vec{\nabla}\vec{B}-\nabla\left(\frac{B^2}{8\pi}\right), \quad (10)$$

where ρ is the gas density; $\vec{v}_0$, the velocity of the fluid; P, the pressure; $\vec{F}$, the total force due to gravity and $\vec{B}$, the magnetic field. We assume standard MHD conditions i.e. infinite conductivity. Equation (10) is simplified by assuming axisymmetry and assuming pure rotation, where $\vec{v_0} = (v_{0r}, v_{0\phi}, v_{0z}) = (0, \theta, 0)$ even if these conditions are not necessary regarding the dynamic effects in the radial direction. Taking into account all these facts, the motion equation in the radial cylindrical coordinate is

$$\rho\left(-\frac{d\Phi(r)}{dr}+\frac{\theta^2}{r}\right)-\frac{dP}{dr}-F_r^{mag}=0, \quad (11)$$

where $\Phi(r)$ is the gravitational potential; F_r^{mag}, the radial component of the magnetic force, and P the pressure of the fluid. We can assume that pressure gradients in the radial direction are negligible (Battaner & Florido 2000). In this case, then the radial component of the magnetic force is given by

$$F_r^{mag}=\frac{1}{4\pi}\left(\frac{B_\phi^2}{r}+\frac{1}{2}\frac{dB_\phi^2}{dr}\right), \quad (12)$$

and the contribution of the magnetic field to the circular velocity is given by

$$v_{mag}^2=\frac{r}{4\pi\rho}\left(\frac{B_\phi^2}{r}+\frac{1}{2}\frac{dB_\phi^2}{dr}\right). \quad (13)$$

3.3. Modelling the rotation curve

The rotation curve is obtained, as usual, by quadratic summation of the different contributions

$$\theta(r)^2 = v_b(r)^2+v_d(r)^2+v_h(r)^2+v_{mag}(r)^2, \quad (14)$$

where we explicitly set $v_b(r) = 0$ as mentioned above.

3.4. Model selection

For the luminous mass models, the different parameters are considered as fixed values in our analysis (see Table 1). For the NFW dark halo, we constrain the V_{200} and c parameters, allowing a range for V_{200} between 100 and 220 km/s with steps of 0.5 km/s and $c \in [5, 30]$ with steps of 0.3. The contribution of the magnetic field to the rotation curve is fitted through one free parameter, r_1, that we are considering which is equivalent to fit B_ϕ as we discussed above. For this parameter, we have explored values in the range from 1 to 1000 kpc. Our analysis is based on a reduced-χ^2 as the goodness-of-fit statistic. Thus, the best-fit parameters are obtained by minimizing this function

$$\chi^2=\frac{1}{N-M}\sum_{i=1}^{n}\frac{(\theta_i^{obs}-\theta_i^{model})^2}{\sigma_i^2}, \quad (15)$$

where N is the total number of points to which we have measured the rotational velocity and depends on the considered dataset ($N = 74$ for C09 and $N = 27$ for C10) and M is the number of free parameters. The sum runs over the observational data points, being θ_i^{obs} the observed velocity and θ_i^{model} the modelled velocity, which depends on the particular model. We shall consider two models: one without magnetic contribution (DM) and another with the magnetic field (DM+MAG). Finally, σ_i is the observational error bar associated to each data point.

4. Results and discussion

Our main results are summarized in Figure 1. The dotted line shows our best-fit rotation curve

Dataset	Disc parameters
C09	$R_d = 5.6$ kpc
	$M_d = 7.1 \times 10^{10}\ M_\odot$
	$M_{gas} \sim 6.6 \times 10^9\ M_\odot$
C10	$R_d = 4.5$ kpc
	$M_d = 8.0 \times 10^{10}\ M_\odot$
	$M_{gas} \sim 7.7 \times 10^9\ M_\odot$

Table 1: Fixed parameters for bulge and disc.

for C09 and C10 when considering only the usual dynamical components (the stellar component and the dark halo at this range of distances), while the solid line shows the result when adding up also the magnetic contribution.

The most important result is that, as shown in Battaner & Florido (2000), the effects of magnetism on the rotation curve are only relevant at large radii (in this case of M31, at distances larger than about 25 kpc). In this sense, the radial range of the datasets of C09 and C10 are optimal to observe the magnetic effects.

Table 2 summarizes our results for the best-fit solutions without (labelled as DM model) and with magnetic field influence (DM + MAG model). As shown, magnetic effects on the gaseous disc significantly decrease the value of the reduced χ^2 statistic for both datasets. Specially for C09, the fit is significantly improved when taking into account a new parameter ($\Delta\chi^2 = 6.5$). The radial scale factor of the magnetic field (r_1) is unconstrained in both cases, but shows clear preference for high values, which means that the best-fit solution for the field slowly decreases with the radial distance in the considered interval (i.e. between 10 and 38 kpc). For example, at $r \sim 38$ kpc, the field is found to be $B_\phi \gtrsim 4.4$ μG for C09 and $B_\phi \gtrsim 4.0$ μG for C10 for this best-fit solution. Both values are compatible with the strength of the field obtained by Fletcher et al. (2004) who found a nearly constant strength of the regular field of about $\sim 5\mu$G between 6 kpc and 14 kpc. Moreover, when no radial variation of the strength is considered, (i.e. if $r_1 \to \infty$), and we fit for the amplitude B_ϕ, we obtain that $B_\phi = 4.7^{+0.6}_{-0.7}$ μG which it is again compatible with results discussed above. This suggests that the data do not require an important radial variation of the strength of the field for the considered range of distances, or in other words, the contribution of the second term in the r.h.s. of Equation (12) is negligible (i.e. $dB_\phi^2/dr \ll B_\phi^2/r$). Therefore, if we had considered another radial profile (e.g. exponential), we would have found a large radial scale factor too. The azimuthal component of the field is practically constant between 10 and 38 kpc.

Our results imply large magnetic fields at large radii. How these are produced lies beyond our scope. On the other hand, we would expect the extragalactic field to be also of this order of magnitude. Theoretical predictions (Dar & de Rújula 2005) suggest values of the level of few μG for the intergalactic magnetic fields (hereafter IGMF). Kronberg (1994); Govoni & Feretti (2004); Kronberg (2005) have reviewed observations of μG level in rich clusters, though no direct measurements have been reported for the IGMF in the Local Group near M31. The observational evidence for IGMF is still weak, but quite strong IGMF near galaxies cannot be disregarded.

We finally note the apparent discrepancy between our derived parameters for the DM model and those obtained by C09 and C10 (see Sect. 2.2). However, it is important to stress that we are restricting the fit to the outer region of M31 ($r >$ 10 kpc). In this outer range, there is a weaker dependence of the shape of the rotation curve on the concentration parameter c, and thus lower values of c are found because the fit tries to compensate the rising behaviour in the outer part. The inclusion of the magnetic field corrects this apparent discrepancy, and in this case the values of c are now compatible with those obtained by C09 and C10.

5. Conclusions

The rotation curve of M31 (Chemin et al. 2009; Corbelli et al. 2010) is rather representative of the standard rotation curves of spirals for $r < 30$ kpc, but it seems to rise out to, at least 38 kpc, the limiting distance of the observations. Indeed, this behaviour is not restricted to M31, and we are probably dealing with a common dynamical feature of many other spirals. Therefore, the outermost rising rotation curve is a very important theoretical challenge.

It is certainly a challenge as the standard dark matter halo models, in particular the universal NFW profiles, do not account for this dynamical unexpected behaviour.

A conventional galactic model, with bulge, disc and dark matter halo, has been shown to provide good fit to the data in the range $r < 20$ kpc (C09, C10). Here, we take advantage of these results and we do not fit any of the luminous components, which are taken to be exactly the same as those proposed by C09 and C10. We have restricted our study to the region $r > 10$ kpc, and we only fitted the parameters describing the dark matter halo, and the magnetic field contribution. Our main conclusion is that magnetic fields are not ignorable for explaining large-scale dynamic phenomena in M31, producing a significant improvement of the fit of the rotation curve at large distances. Moreover, the required field strength of the regular component ($B_\phi \sim 4$ μG) is fully consistent with the measured magnetic field in M31 at least up to $r \sim 15$ kpc.

This conclusion seems very reasonable, as magnetic fields are amplified and act "in situ", and therefore they become increasingly important at the rim, where gravity becomes weaker.

The best-fit model of the magnetic fields requires a field strength slowly decreasing with radius. This slow decrease is compatible with present values of the strength derived from observations of the polarized synchrotron emission of the disc, but clearly we need measurements of Faraday rotation of extragalactic sources at this large radii to confirm that the magnetic field is present up to this distance and to trace unambiguously the regular component. Hence, future experiments such as LOFAR[1] and SKA[2] (Beck 2009), will be extremely important, allowing a detailed explorations on the galactic edge as well as in the intergalactic medium.

Model	Parameters	C09	C10
DM	V_{200} (km/s)	160.2 ± 2.0	$132.1^{+5.7}_{-5.4}$
	c	12.3 ± 0.6	$19.1^{+2.4}_{-2.2}$
	χ^2	19.8	1.1
DM + MAG	V_{200} (km/s)	$133.8^{+1.7}_{-1.3}$	$120.0^{+4.7}_{-4.0}$
	c	$22.7^{+1.2}_{-1.1}$	$25.0^{+2.8}_{-2.9}$
	r_1 (kpc)	> 888.0	> 185.0
	χ^2	13.3	0.6

Table 2: Best-fit for the rotation curve with and without the contribution of magnetic fields for $r \gtrsim 10$ kpc.

This work was partially supported by projects AYA2007-68058-C03-01 of Spanish Ministry of Science and Innovation (MICINN), by Junta de Andalucía Grant FQM108 and by Spanish MEC Grant AYA 2007-67625-C02-02. JAR-M is a Ramón y Cajal fellow of the MICINN.

REFERENCES

Battaner, E., Garrido, J. L., Membrado, M., & Florido, E. 1992, Nature, 360, 652

Battaner, E. & Florido, E. 1995, MNRAS, 277, 1129

Battaner, E. 1996, Astrophysical Fluid Dynamics, by E. Battaner, pp. 256. ISBN 0521431662. Cambridge, UK: Cambridge University Press, March 1996.

Battaner, E. & Florido, E. 2000, Fundamentals of Cosmic Physics, 21, 1

Battaner, E. & Florido, E. 2007, Astronomische Nachrichten, 328, 92

Beck, R. 1982, A&A, 106, 121

Beck, R., Brandenburg, A., Moss, D., Shukurov, A., & Sokoloff, D. 1996, ARA&A, 34, 155

Beck, R. 2001, Space Science Reviews, 99, 243

[1] http://www.lofar.org

[2] http://www.skatelescope.org/

Beck, R. 2004, Ap&SS, 289, 293

Beck, R. 2005, Cosmic Magnetic Fields, 664, 41

Beck, R. 2007, A&A, 470, 539

Beck, R. 2009, IAU Symposium, 259, 3

Beck, R. 2009, Revista Mexicana de Astronomia y Astrofisica Conference Series, 36, 1

Berkhuijsen, E. M., Beck, R., & Hoernes, P. 2003, A&A, 398, 937

Binney, J., & Tremaine, S. 1987, Princeton, NJ, Princeton University Press, 1987, 747 p.

Braun, R. 1991, ApJ, 372, 54

Braun, R., Thilker, D. A., Walterbos, R. A. M., & Corbelli, E. 2009, ApJ, 695, 937

Chemin, L., Carignan, C., & Foster, T. 2009, ApJ, 705, 1395

Corbelli, E., Lorenzoni, S., Walterbos, R., Braun, R., & Thilker, D. 2010, A&A, 511, A89 (C10)

Dar, A., & de Rújula, A. 2005, Phys. Rev. D, 72, 123002

de Blok, W. J. G., Walter, F., Brinks, E., Trachternach, C., Oh, S.-H., & Kennicutt, R. C. 2008, AJ, 136, 2648

Fardal, M. A., Babul, A., Geehan, J. J., & Guhathakurta, P. 2006, MNRAS, 366, 1012

Fletcher, A., Berkhuijsen, E. M., Beck, R., & Shukurov, A. 2004, A&A, 414, 53

Freeman, K. C. 1970, ApJ, 160, 811

Geehan, J. J., Fardal, M. A., Babul, A., & Guhathakurta, P. 2006, MNRAS, 366, 996

Govoni, F., & Feretti, L. 2004, International Journal of Modern Physics D, 13, 1549

Han, J. L., Beck, R., & Berkhuijsen, E. M. 1998, A&A, 335, 1117

Hernquist, L. 1990, ApJ, 356, 359

Howley, K. M., Geha, M., Guhathakurta, P., Montgomery, R. M., Laughlin, G., & Johnston, K. V. 2008, ApJ, 683, 722

Ibata, R., Irwin, M., Lewis, G., Ferguson, A. M. N., & Tanvir, N. 2001, Nature, 412, 49

Kassin, S. A., de Jong, R. S., & Weiner, B. J. 2006, ApJ, 643, 804

Kronberg, P. P. 1994, Reports on Progress in Physics, 57, 325

Kronberg, P. P. 2005, Cosmic Magnetic Fields, 664, 9

Kutschera, M., & Jalocha, J. 2004, Acta Physica Polonica B, 35, 2493

Navarro, J. F., Frenk, C. S., & White, S. D. M. 1996, ApJ, 462, 563

Navarro, J. F., Frenk, C. S., & White, S. D. M. 1997, ApJ, 490, 493

Nelson, A. H. 1988, MNRAS, 233, 115

Noordermeer, E., van der Hulst, J. M., Sancisi, R., Swaters, R. S., & van Albada, T. S. 2007, MNRAS, 376, 1513

Ruiz-Granados, B., Rubino-Martin, J. A., & Battaner, E. 2010, arXiv:1006.5573

Seigar, M. S., Block, D. L., Puerari, I., Chorney, N. E., & James, P. A. 2005, MNRAS, 359, 1065

Spano, M., Marcelin, M., Amram, P., Carignan, C., Epinat, B., & Hernandez, O. 2008, MNRAS, 383, 297

Stepanov, R., Arshakian, T. G., Beck, R., Frick, P., & Krause, M. 2008, A&A, 480, 45

Tsiklauri, D. 2008, arXiv:0806.1513

Walterbos, R. A. M., & Kennicutt, R. C., Jr. 1987, A&AS, 69, 311

This 2-column preprint was prepared with the AAS LaTeX macros v5.2.

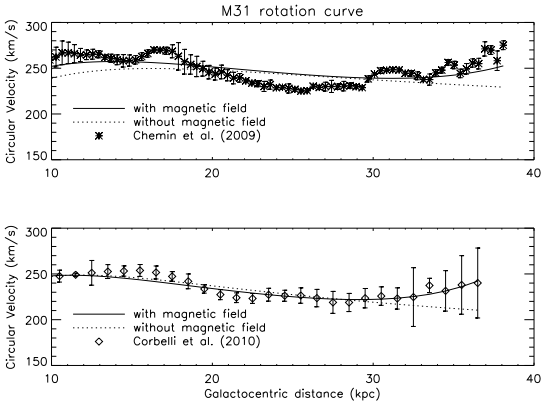

Fig. 1.— Best-fit solutions for the rotation curve of M31, with and without including the contribution of a regular magnetic field component. Top shows the C09 dataset and bottom the C10 dataset. Asterisks and rombhus represent the observational data with the associated error bars. The solid line is the best fit derived in this paper, including the contribution of the regular magnetic field over the gaseous disc. The dotted line is the best-fit model obtained without the contribution of the magnetic field.